Metastable Helium Atom Stimulated Desorption of H^+ Ion

Mitsunori Kurahashi and Yasushi Yamauchi
National Research Institute for Metals, 1-2-1 Sengen, Tsukuba, Ibaraki 305-0047, Japan
(Received 15 July 1999)

H^+ desorption induced by the impact of metastable helium atoms has been found for $H_2O/Na/Ni(110)$ coadsorption systems. The measurements were carried out using a time-of-flight technique and a pulsed-discharge type metastable helium atom (He^*) source. It is concluded that the H^+ desorption by He^* is induced by a hole created on the valence levels via the Auger deexcitation of He^*. The H^+ desorption by He^* may be understood within the framework of the Menzel-Gomer-Readhead model.

PACS numbers: 79.20.Rf, 78.70.–g, 79.20.La, 79.60.–i

The interaction of metastable rare gas atoms with solid surfaces has attracted considerable interest over the last two decades. As metastable atoms moving at a thermal energy cannot penetrate the surface, the electrons ejected by the impact of the metastable atom provide information on the electronic states of the outermost surface [1,2]. This analytical technique, known as metastable deexcitation spectroscopy (MDS or MIES), has been applied to the study of various surfaces [1,2]. Recently, another promising feature has been revealed, i.e., that the electronic transition induced by the metastable atom can cause damage to the self-assembled monolayer of organic molecules, and the potential of the metastable atom beam as a tool for future lithography has been discussed [3]. Considering the results of these studies, it is quite reasonable to expect that the desorption induced by electronic transitions (DIET) may occur by the impact of metastable atoms.

In the present study, we observed H^+ desorption induced by the metastable helium atom (He^*) for $H_2O/Na/Ni(110)$ coadsorption systems. [This phenomenon might be termed metastable-atom stimulated desorption (MSD).] It is concluded that the H^+ MSD is induced by a hole created on the valence levels via the Auger deexcitation of He^*. As the hole is created only on the outermost surface, it is considered that the desorbed ion derives only from the outermost surface.

Our experiments were conducted in an ultrahigh vacuum chamber (base pressure of 1.4×10^{-10} Torr) equipped with a He^* source [4], a rotatable 180° electrostatic energy analyzer, a LEED-AES optics, a sputter ion gun, and a Stern-Gerlach analyzer. The primary beam was generated by operating the He^* source in the pulsed discharge mode [4] with an average discharge current of 2 mA. The discharge pulse width was 10 μS and its repetition rate was 1.8 kHz. The primary beam, which contains He^*, ultraviolet photons, and fast neutral He atoms [4], was directed onto the sample with an incidence angle of 30° to the surface normal. Electrons and positive ions ejected perpendicularly to the sample surface were detected by the electrostatic energy analyzer, and their time-resolved intensities were measured by a multichannel scaler. When the positive ions were detected, the sample was positively biased to enhance their collection efficiency. The neutral species were detected by an additional channel electron multiplier (CEM). Charged particles were removed by a deflector and a grid located in front of the CEM entrance. The beam diameter on the sample was about 4 mm, and the sample current during the primary beam irradiation was 20 pA for the clean Ni(110) surface. Stern-Gerlach analysis indicated that the relative intensity of $He^*(2^3S)$ and $He^*(2^1S)$ in the primary He^* beam was 9:1. The MDS and ultraviolet photoelectron spectroscopy (UPS) spectra were measured using the same pulsed discharge source and timing electronics.

A clean Ni(110) surface was prepared by repeated annealing and Ar^+ sputtering. One monolayer of Na atoms was deposited on the clean Ni(110) surface at 298 K from the SAES Getters source. Na coverage was estimated based on the work function and MDS spectra measured as a function of the Na deposition time.

Figure 1 shows the time-resolved intensities of positive ions, neutrals, and secondary electrons. The horizontal axis corresponds to the arrival time of these particles, which represents the sum of the flight time of the primary and ejected (or scattered) particles. The arrival time distribution of the ejected secondary electrons corresponds to the time-of-flight (TOF) distribution of the primary particles because the flight time of secondary electrons is negligibly short. A broad peak at 100–300 μS is due to the primary He^*, and its kinetic energy is found to be 50–250 meV from its TOF distribution. A peak at 0–10 μS is due to the primary photon and fast He. The TOF distribution of the neutrals shows prominent features at 0–20 μS, which are due to the reflected photon and fast He atom. The reflected photon contributes to the spectrum at 0–10 μS, at which the discharge is on. Therefore, the two sharp peaks at 10 and 20 μS are expected to be due to the scattered fast He atoms. Since their time separation of $\sim$10 μS coincides with the discharge pulse width, the peak at $\sim$10 μS may correspond to the fast He atoms generated at the rising edge of the discharge pulse and the peak at $\sim$20 μS to those generated at the down edge. Their kinetic energies, estimated based on this peak assignment, are $\sim$80 eV. Note that their electronic states have been

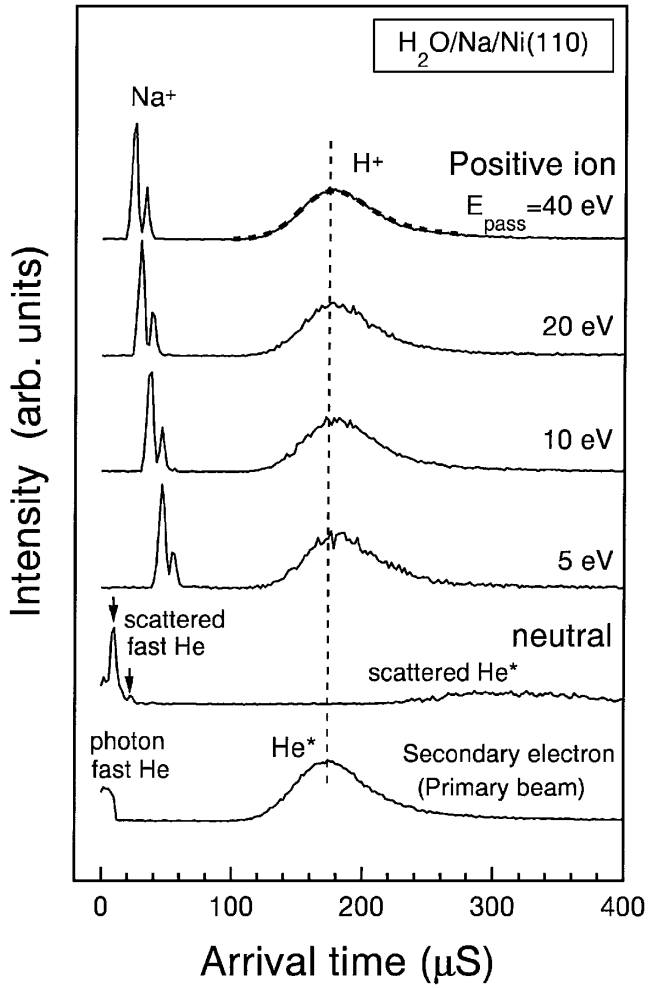

FIG. 1. The time-resolved intensities of secondary electrons with a kinetic energy of 3.1 eV, neutrals and positive ions measured at the H_2O exposure of 4.1 L. The positive ions with a kinetic energy of 103 eV were monitored for the positively biased sample (+100 V) with the analyzer pass energies (E_{pass}) shown. The primary He^* peak shifted to match the H^+ peak is shown in the dashed line.

found to be ground state, which will be discussed elsewhere. A broad peak at 200–400 μS corresponds to the scattered He^* atoms.

The time-resolved spectra of desorbed positive ions show distinct peaks at 20–60 μS and 100–300 μS. Their positions are shifted by changing the analyzer pass energy (E_{pass}). This results from the increase in the flight time of the desorbed ions in the energy analyzer by decreasing E_{pass}. Actually, linear relationships have been found for the plots of their peak positions versus $1/\sqrt{E_{\text{pass}}}$. From the slope of the plots, the first peak has been assigned to Na^+ and the second peak to H^+. The first peak exhibits a doublet structure and its shape is kept unchanged with the change in E_{pass}. This indicates that the doublet structure originates from the same species (Na^+) desorbed at a different time. As mentioned above, a similar doublet structure is observed for the scattered fast He atoms, indicating that the Na^+ ions are desorbed by the fast He atoms. The position of the H^+ peak converges to that of the primary He^* with increasing E_{pass}. It is therefore concluded that the H^+ ion is desorbed by the primary He^*. Figure 1 shows that the shape of the H^+ peak almost coincides with that of the primary He^*, indicating that the H^+ desorption yield is nearly constant at the kinetic energy range of 50–250 meV.

Figure 2 shows the energy distribution of the desorbed positive ions. Since ions ejected along the surface normal are detected for the positively biased sample, the collection efficiency for low energy ions may be enhanced. The energy distribution of Na^+ is characterized by the high-energy tail. This is a common feature of secondary ions ejected via collisional sputtering [5]. On the contrary, no high-energy tail is observed for H^+. This reflects the fact that the H^+ MSD is not due to collisional processes.

Figure 3 shows the MDS and UPS spectra measured for the $H_2O/Na/Ni(110)$ surface. Before discussing the MDS spectra, the He^* decay mechanism is briefly explained. Since the work function of the present surface is sufficiently low, He^* decays via Auger deexcitation (AD) [1] or autodetachment [2,6] processes. In the AD process, a surface electron fills the $1s$ hole of He^*, and the $2s$ electron of He^* is ejected. If the work function is lower than the affinity level of He^*, the surface electron may tunnel into the He^* $2s$ level, and the resultant He^- decays to the ground state He atom, ejecting an electron (autodetachment). Since these two processes involve one surface electron, the MDS spectra exhibit UPS-like features. Figure 3 shows three MDS peaks (A–C). Peak A is assigned to Na $3s$ states. It decays with increasing H_2O exposure and disappears at around 1 L. He^* decays via the AD or autodetachment processes when it ejects an electron

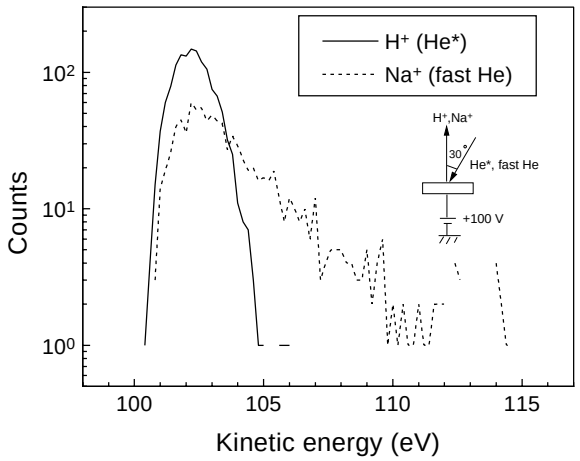

FIG. 2. The energy distribution of H^+ desorbed by He^* and Na^+ desorbed by fast neutral He atoms measured at the H_2O exposure of 4.1 L with $E_{\text{pass}} = 10$ eV (the energy resolution of 1 eV). Because the contact potential difference between the sample and the analyzer (~1 eV) is not corrected, the spectra are shifted to higher kinetic energy.

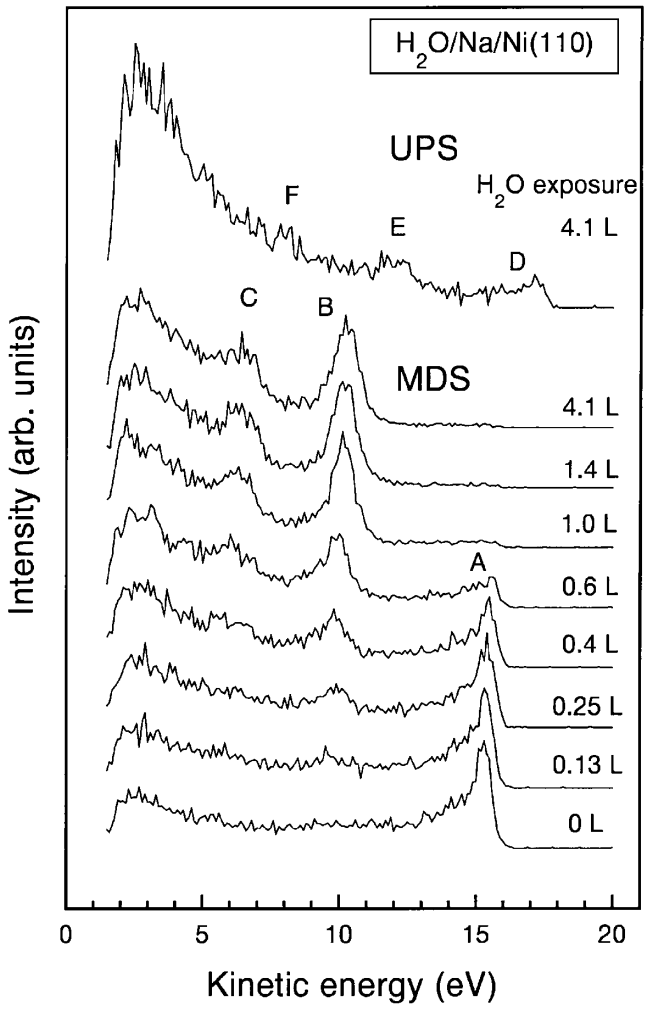

FIG. 3. The MDS and UPS spectra of the H_2O/Na/Ni(110) surface measured at the H_2O exposure shown.

corresponding to peak *A*. The intensities of peaks *B* and *C* increase with the increase of the H_2O exposure and become dominant at exposures >1 L. Peaks *B* and *C* correspond to the binding energies (E_B) of 5–6 eV and 9–10 eV, respectively, agreeing well with those reported for H_2O/Na/transition metal coadsorption systems [7]. It has been reported that H_2O dissociatively adsorbs on the Na-deposited surface, and the energy levels at $E_B = 5$–6 eV and 9–10 eV have been assigned to the 1π and 3σ orbitals of the OH group [7]. He^* decays via the AD mechanism when it ejects electrons corresponding to these two levels. The UPS spectrum shows three peaks. The UPS peaks *E* and *F* are located about 2 eV above the MDS peaks *B* and *C*. Since this energy difference is close to the difference in the excitation energy of He^* 2^3S (19.8 eV) and the He I photon (21.2 eV), peaks *E* and *F* correspond to the same energy levels as peaks *B* and *C*, respectively. Because no corresponding MDS peak is observed, peak *D* is due to electrons at subsurface regions.

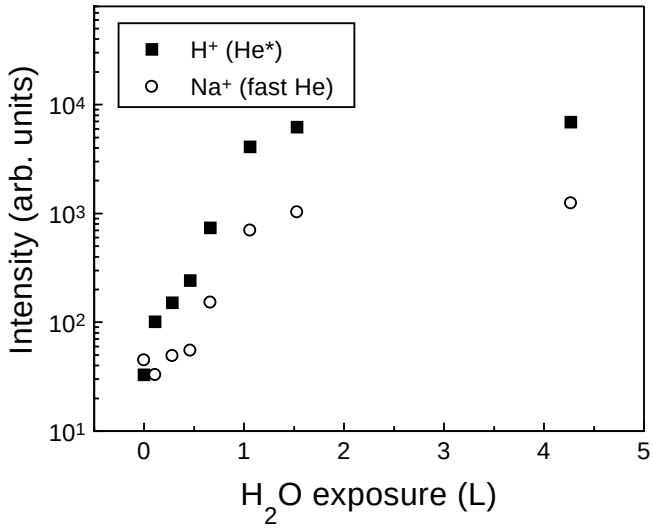

FIG. 4. The intensities of the desorbed H^+ and Na^+ ions as a function of the H_2O exposure.

Figure 4 shows the change in the intensities of desorbed H^+ and Na^+ ions with H_2O exposure. Two important features are found in this result. The first one is a steep increase in the Na^+ and H^+ intensities at 0.5–1 L. This can be understood from the behavior of the Na 3*s* states. Figure 3 shows that the Na 3*s* states disappear at 0.5–1 L, which causes the steep decrease in the neutralization rate of ions. Therefore, the steep increase in the desorption yields originates from the steep decrease in the neutralization rate of desorbed ions. This suggests that hydrogen is also desorbed as a neutral atom by He^*. The second important feature is the difference in the behavior of the Na^+ and H^+ desorption rate at lower exposures. The Na^+ intensity is nearly constant at <0.5 L, while the H^+ intensity increases with increasing H_2O exposure. This may result from the fact that the concentration of Na is almost constant while that of H increases with increasing the H_2O exposure.

The mechanism for H^+ MSD is discussed below. As noted above, He^* decays via the AD or autodetachment processes. Both processes create one hole on the outermost surface and eject the He^* 2*s* electron. Therefore, either the ejected 2*s* electron or the hole induces the H^+ MSD. The desorption mechanism involving the ejected electron can be excluded for the following reasons. The energy of the electrons ejected by He^* is lower than that of the electrons ejected by the primary photon (21.2 eV) because the excitation energy of He^* is lower than that of the photon. Figure 3 clarifies this for the present surface. Therefore, if we assume that H^+ desorption is induced by the ejected electron, the photon-stimulated desorption (PSD) of H^+ must be observed. Furthermore, the H^+ PSD and MSD yields must be roughly proportional to the intensities of electrons ejected by the primary photon and He^*, which are shown in Figs. 1 and 3. No H^+ PSD signal, however, is observed in spite of the presence of the large H^+ MSD

peak (Fig. 1). This leads to the conclusion that the H^+ MSD is not induced by the ejected $2s$ electron but by the hole created by He^*. It should be emphasized that the hole is created only at the outermost surface.

The energy level of the hole created via the AD process (E_B) may satisfy the condition $E_{\rm kin} = E_{\rm ex} - E_B - \phi_S > 0$. Here, $E_{\rm kin}$ is the kinetic energy of the ejected $2s$ electron, $E_{\rm ex}$ is the excitation energy of He^*, and ϕ_S is the work function of the surface. $E_{\rm ex}$ is 20.6 eV for He^* 2^1S and 19.8 eV for He^* 2^3S. Since ϕ_S at the H_2O exposure of 4.1 L was found to be about 3 eV, E_B should be less than 18 eV, indicating that core levels such as Na $2p$ and O $2s$ states are not involved in the H^+ MSD. It is therefore concluded that the H^+ MSD is induced by a hole created on the valence levels observed by the MDS measurement (peaks A–C).

The H^+ MSD may be understood within the framework of the Menzel-Gomer-Readhead (MGR) model [8,9]. If He^* extracts a bonding electron from the H-surface (H-S) bond, the bond becomes weaker, and the H-S equilibrium distance thus becomes longer. This means that the AD process which extracts a bonding electron induces a transition from the H-S ground state potential to the repulsive part of the potential for the $[H\text{-}S]^+$ system. If the potential at the transition point is sufficiently high, the H atom desorbs as a neutral H atom or H^+. Figure 3 shows that two MDS peaks are observed at H_2O exposure of 4.1 L. As mentioned above, these states correspond to the 1π ($E_B = 5$–6 eV) and 3σ ($E_B = 9$–10 eV) orbitals of the O-H bond. Because at least the latter orbital is bonding, the H^+ MSD can be caused by the creation of a hole on it. Future discussions will benefit from information on the potential energy curve for the adsorbed $[OH]^+$. The use of other metastable rare gas atoms, which have different excitation energies, will enable us to specify the holes responsible for the H^+ MSD. Note that no MSD peaks due to O^+ and OH^+ are observed. Because oxygen is expected to be at least O^- and more likely O^{2-} on the present surfaces, a process which creates at least two holes must be involved for the formation of these species. The AD process, however, creates only one hole. This explains the absence of the O^+ and OH^+ MSD peaks.

In regard to the H^+ desorption mechanism mentioned above, we note the following. We have proposed a mechanism via the hole creation on the valence levels by He^*. Although the primary photon can also create a hole on the same levels, H^+ PSD is not observed. A possible explanation for this is as follows. He^* decays on the outermost surface while the He I photon penetrates over 100 atomic layers. This means that the probability for ionizing the atoms on the outermost surface is nearly unity for He^* and much smaller for the photon. In addition, the ion desorption probability is the largest for the ions present at the outermost surface [9]. The MSD ion yield is therefore expected to be much higher than the PSD ion yield. Moreover, the ionization cross section of the H atom by He^* may differ from that by the photon because of the difference between the electron-electron and electron-radiation interactions. This can contribute to the difference in the H^+ PSD and MSD yields.

In summary, H^+ desorption by the impact of He^* with a thermal kinetic energy has been observed for $H_2O/Na/Ni(110)$ coadsorption systems. It has been concluded that H^+ desorption is induced by a hole created on the valence levels via the Auger deexcitation of He^*. Unlike ESD and PSD, which involve an appreciable contribution from deeper layers [9], MSD has the potential to provide selective information on the surface-adsorbed species.

[1] H. Conrad, G. Ertl, J. Küppers, W. Sesselmann, and H. Haberland, Surf. Sci. **121**, 161 (1982); W. Sesselmann, B. Woratschek, J. Küppers, G. Ertl, and H. Haberland, Phys. Rev. B **35**, 1547 (1987); **35**, 8348 (1987).

[2] Y. Harada, S. Masuda, and H. Ozaki, Chem. Rev. **97**, 1897 (1997).

[3] A. Bard, K. K. Berggren, J. L. Wilbur, J. D. Gillaspy, S. L. Rolston, J. J. McCelland, W. D. Phillips, M. Prestiss, and G. W. Whitesides, J. Vac. Sci. Technol. B **15**, 1805 (1997); S. Nowak, T. Pfau, and J. Mlynek, Appl. Phys. B **63**, 203 (1996). The metastable-atom lithography on hydrogen-passivated silicon surfaces is also described in S. B. Hill, C. A. Haich, F. B. Dunning, G. K. Walters, J. J. McClelland, R. J. Celotta, and H. G. Craighead, Appl. Phys. Lett. **74**, 2239 (1999).

[4] Y. Yamauchi, M. Kurahashi, and N. Kishimoto, Meas. Sci. Technol. **9**, 531 (1998); M. Kurahashi and Y. Yamauchi, Surf. Sci. **420**, 259 (1999).

[5] J. C. Vickerman, in *Secondary Ion Mass Spectrometry,* edited by J. C. Vickerman, A. Brown, and N. M. Reed (Clarendon, Oxford, 1989), p. 22.

[6] R. Hemmen and H. Conrad, Phys. Rev. Lett. **67**, 1314 (1991); Appl. Phys. A **55**, 411 (1992).

[7] J. Paul, Surf. Sci. **160**, 599 (1985); S.-A. Lindgren, J. Paul, and L. Wallden, Surf. Sci. **155**, 165 (1985); P. A. Thiel and T. E. Madey, Surf. Sci. Rep. **7**, 211 (1987).

[8] R. D. Ramsier and J. T. Yates, Jr., Surf. Sci. Rep. **12**, 243 (1991).

[9] M. Akbulut, N. J. Sack, and T. E. Madey, Surf. Sci. Rep. **28**, 177 (1997).